Influence of Geometrical Configuration of a Translucent Fiberglass Post on the Polymerization of a Dual Cure Resin Cement Analyzed by EPR Spectroscopy

Bruno Luiz Santana Vicentin[1] · **Fabio Martins Salomão**[2] ·
Márcio Grama Hoeppner[2] · **Eduardo Di Mauro**[1]

Abstract   This research aimed to study the influence of the geometrical configuration of a translucent fiberglass post on the dual cure resin cement polymerization by electron paramagnetic resonance (EPR) spectroscopy. A 20-mm long, White Post DC no. 1 fiberglass post (FGM, Joinvile, SC, Brazil) was sectioned in half to obtain two different groups of posts: cylindrical and conical. Each post was cemented with AllCem A1 dual cure resin cement (FGM, Joinvile, SC, Brazil) using a root canal model and light cured for 40 s. Following cementation, the post was removed and sectioned to obtain 2 mm samples at different depth of cementation. EPR spectra were obtained 10 min and 24 h after cementation to determine the concentration of free radicals (FR) in the surrounding hardened (cured) dental cement, once the concentration of FR is proportional to the light intensity at the restoration point. No significant decrease was observed in light transmission through the cylindrical post that affected the FR concentration, at depths up to 5.5 mm. In contrast, a decrease was verified for all samples conical geometry. The light conduction was effective up to 5.5 mm of curing depth when a cylindrical post was used. The cylindrical configuration was more efficient at conducting light to the deepest points of the restoration compared with the conical configuration.

✉ Eduardo Di Mauro
  dimauro@uel.br

[1]   Department of Physics, State University of Londrina, Londrina 86057-970, Brazil

[2]   Department of Restorative Dentistry, State University of Londrina, Londrina 86057-970, Brazil

1 Introduction

Intraradicular posts manufactured from a composite of glass fibers and epoxy resin are often used in the treatment of teeth for the purpose of assisting the retention of the restoration material [1–4]. The fiberglass post became popular in dental practice because of its physical properties, which are very similar to dentin, for its adhesion to root dentin and its esthetic qualities, which differ considerably from the cast metal post [5]. The retention of the fiberglass post with resin material directly depends on the degree of conversion of the cement selected, which can be polymerized by mixing the base paste and a catalyst (chemical initiation), or by blue visible light irradiation (photoinitiation, wavelength between 400 and 500 nm) associated with chemical initiation (double-polymerized/dual-cured) [6–8].

In dual-cured resin cements, the incident light interacts with camphorquinone, which reacts with a tertiary amine, resulting in the formation of reactive free radicals (FR) that are responsible for the conversion of monomers to polymers [3, 9]. Thus, translucent fiberglass posts were developed for the purpose of transmitting light and improving cement polymerization throughout the length of the root canal [6, 10]. The efficiency of light transmission by the post, and hence the improvement in the degree of resin cement conversion, is directly proportional to the post diameter [11]. Incomplete polymerization compromises the mechanical properties of the composite material, which means that a clear understanding of the polymerization process is important [10, 12, 13].

The degree of conversion is related to the amount of FRs generated during resin polymerization. Electron paramagnetic resonance (EPR) spectroscopy is a highly sensitive technique for identifying and quantifying the concentration of FRs without any changes in the material composition, including those used in the fiberglass post cementation [14–18]. Since the signal intensity is proportional to the amount of paramagnetic species in the sample, this spectroscopic technique is adequate in this research, where minor variations in the generation of FRs can be detected.

This research aimed to evaluate the influence of the geometrical configuration of a translucent White Post no. 1 fiberglass post (FGM, Joinvile, SC, Brazil) on the polymerization of AllCem A1 dual cure resin cement (FGM, Joinvile, SC, Brazil). The relative concentration of FRs generated in the resin cement was analyzed by EPR spectroscopy in X-band separately for the cylindrical and conical parts of the surrounding hardened (cured) dental cement at different depths. The relationship between post shape and FR concentration in different sections was verified for each post shape.

2 Materials and Methods

2.1 Experimental Design

This experiment aimed to evaluate the relative concentration of FRs in samples from the dual cure resin cement Allcem (FGM, Joinville, SC, Brazil) of shade A1 by

Table 1 Experimental groups and material evaluated

Group	Sample	Curing protocol	Factor assessed
G1			
Three cylindrical translucent fiberglass posts, White Post DC (FGM), no. 1 (ClP-1)	Three sections of the cervical quarter Three sections of the middle quarter Three sections of the deep quarter Three sections of the apical quarter	Cement light cured for 40 s	Relative concentration of FR of the cement AllCem (FGM) at two moments in time: T_{10min} after mixing the cement; and T_{24h} after
G2			
Three conical translucent fiberglass posts, White Post DC (FGM), no. 1 (CnP-1)	Three sections of the cervical quarter Three sections of the middle quarter Three sections of the deep quarter Three sections of the apical quarter	Cement not light cured	

electron paramagnetic resonance (EPR) at different restoration points after cementation of a prefabricated translucent fiberglass post White Post DC no. 1 in a simulated root canal (Table 1). The post was sectioned to obtain cylindrical and conical samples in order to study the influence of the geometrical configuration of the translucent fiberglass post in the generation of free radicals, which are known to be responsible for the polymerization of the resin cement. Here cervical means the post part closest to the light source, and apical the farthest part.

The materials used in this experiment have properties and qualities that are very similar to others used worldwide. This methodology provides data and basement to understand the influence of a translucent fiberglass post on the degree of conversion of dual cure resin cement.

After the experimental design to control biases the post allocation in groups, preparing and reading of the samples, all phases of this experiment were randomized.

2.2 Post Sectioning

In order to obtain the samples, three double-tapered (cylindrical and conical) White Post DC (FGM, Joinville, SC, Brazil) no. 1 fiberglass posts, 20 mm in length, were sectioned transversely with a double-sided fine-grained diamond disc (Microdont, Socorro, SP, Brazil), at low speed, obtaining three cylindrical posts no. 1 (ClP-1) and three conical posts no. 1 (CnP-1), 9.5 mm in length.

Likewise, for the construction of the simulated canal for cementing the posts, three double-tapered translucent White Post DC (FGM, Joinville, SC, Brazil)
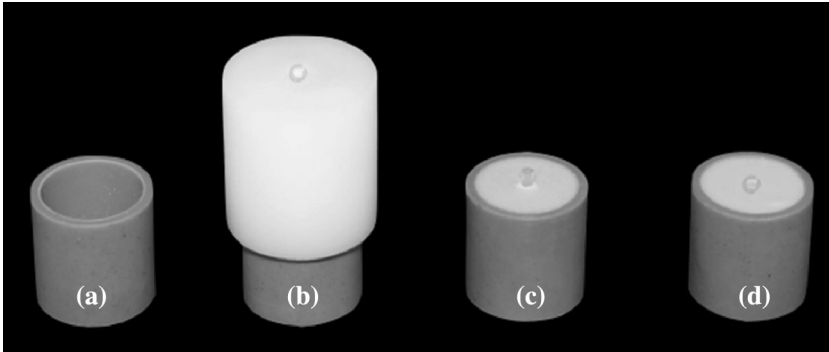
Fig. 1 Matrices and guides system: *a* PVC ring; *b* polyacetal matrix placed over the PVC ring; *c* set PVC, ring, silicon and ClP-3; *d* simulated root canal for post cementation obtained after post removal

fiberglass posts no. 3, 20 mm in length, were cut to obtain three cylindrical fiberglass posts no. 3 (ClP-3) and three conical posts no. 3 (CnP-3), 9.5 mm length.

### 2.3 Obtaining the Guides and Matrices

A PVC (polyvinyl chloride) tube, with an outside diameter of 18 mm, was sectioned using a hydraulic mechanical lathe, to obtain six rings, 8 mm in height (Fig. 1a). A polyacetal matrix, 25 mm in height and 18 mm inner diameter, was fabricated using a hydraulic mechanical lathe. A 2.2-mm diameter hole, 10 mm in depth, was drilled in the center of the polyacetal matrix, along to its long axis. Subsequently, the polyacetal matrix was placed over the PVC ring (Fig. 1b), and Zetalabor (Hard. 85 shore-A, Zhermack, Badia Polesine, Rovigo, Italy) condensation cure silicon putty was inserted on the opposite side. The condensation cure silicon putty was obtained by mixing the base and catalysts, following the manufacturer's recommendations.

The entire internal space was filled and the PVC was positioned under pressure over a glass plate. Posteriorly, ClP-3 was inserted into the polyacetal matrix using a metal rod introduced into the silicon. The entire system (PVC ring, polyacetal matrix, condensation cure silicon and ClP-3) was maintained over the glass plate until the final cure of the silicon. At the end of this stage, the polyacetal matrix was removed, leaving the setting PVC ring, silicon and ClP-3 (Fig. 1c).

Eight millimeters of the ClP-3 were inserted into the modeling material and 1.5 mm remained outside, simulating the clinical process of fiberglass post cementation inside a root canal. The ClP-3 remained in position for 24 h (Fig. 1d). The same protocol was followed for the remaining ClP-3 and CnP-3 posts.

2.4 Obtaining the Samples

The ClP-3 was removed to obtain a cementation path for the ClP-1 in the silicon (Fig. 1d). Likewise, the CnP-3 was removed to obtain a cementation path for the CnP-1. Prior to cementation, the surface of all posts was cleaned with 70 % alcohol
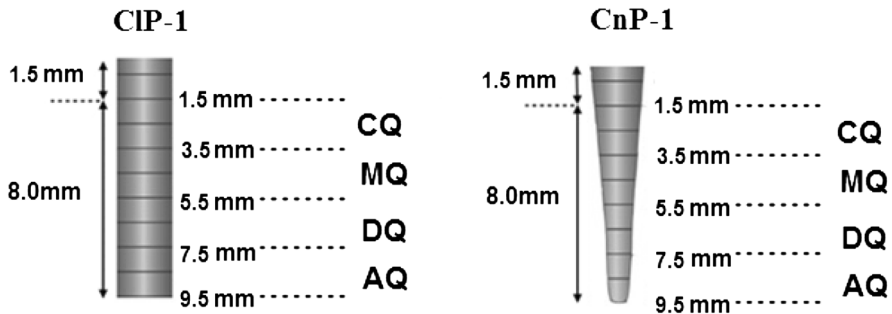
Fig. 2 Schematic representation of samples from ClP-1 (G1) and CnP-1 (G2)

and later, ProsilSilane (FGM, Joinville, SC, Brazil) was applied, waiting 1 min for total evaporation and drying.

The resin cement used was AllCem dual cure resin cement (FGM, Joinville, SC, Brazil), color shade A1, composed of a base paste and catalyst. Disposable auto-mixing points were used, following the manufacturer's recommendation (1:1 by weight). The mixture obtained was inserted into the cementation path in the silicone using a Centrix syringe (DFL, Rio de Janeiro, RJ, Brazil) with the disposable AccuDoseNeedle. Subsequently, ClP-1 and CnP-1 were inserted (cemented) in the condensation cure silicone, along the axis. Any excess cement was removed using a disposable microapplicator (Cavibrush no. 2, FGM, Joinville, SC, Brazil).

After post cementation, the resin cement was photopolymerized for 40 s using a light emitting diode (LED) (Radii Plus-SDI®, São Paulo, SP) with a potency of 1500 mW/cm^2 and in contact with the exposed ClP-1 and CnP-1. Ten minutes after mixing the resin cement, the set ClP-1/CnP-1 and the AllCem cement was removed from the silicone. With a double-sided fine-grained diamond disc (Microdont, Socorro, SP, Brazil) at low speed, the portion of the posts that remained outside following cementation were sectioned, leaving 8 mm corresponding to the cemented part. This part was sectioned every 2 mm to obtain the samples: cervical quarter (CQ, post portion closest to the polymerization device), middle quarter (MQ), deep quarter (DQ) and apical quarter (AQ), with the samples from ClP-1 allocated to Group 1 (G1) and samples from Cn-1 allocated to Group 2 (G2) (Fig. 2). All samples were obtained in the same conditions of light, temperature and oxygen.

2.5 Electron Paramagnetic Resonance Experiment

In this current study, the paramagnetic species are the free radicals generated during the activation stage of the polymerization process of resin cement, and the EPR spectrum was analyzed concerning the signal amplitude to evaluate the relative concentration of free radicals according to the depth of the simulated root canal to characterize the influence of the translucent fiberglass post on the dual cure resin cement polymerization.

Three different free radicals are generated in the methacrylate resin composites (Radical I, Radical II and Radical III), however Radical II does not contribute to the formation of the EPR spectrum because it is too unstable and/or it is generated in a small quantity (Fig. 3). Thus, the nine lines EPR spectrum of methacrylate resins (Fig. 4a) is due to two paramagnetic species simultaneously present in the sample: Radical I (Fig. 3a) and Radical III (Fig. 3b). Fontes et al. showed that the superposition of the nine lines EPR spectrum of Radical I with the five lines EPR spectrum of Radical III results in a nine lines EPR spectrum [19].

Figure 4a shows EPR spectrum of the dual-cured resin cement due to the superposition of Radical I and Radical III [19], and Fig. 4b shows the superposition of EPR spectra with $MgO:Mn^{2+}$ standard for cervical, medium, deep and apical quarters of the conical configuration, and illustrates how the comparison can be done. The first line in the EPR spectrum (Fig. 4b) is the superposition of the third line of the $MgO:Mn^{2+}$ standard with the first line of the resin cement free radical, and the last line in the spectrum is the superposition of the fourth line of the standard with the last line of the free radical. The EPR signal amplitude of free radicals for all groups was normalized with the line intensity of the third line of the $MgO:Mn2^{+}$ standard to compare variances in the intensity of the free radical signal (central line). As cervical quarter showed the most intense EPR signal amplitude and thus the greatest concentration of free radicals, it was taken as the reference point to study the variation on the relative concentration of free radicals between the samples into the group, so that the data presentation is relative to cervical quarter in each group (taken as 100 %).

The EPR spectra in X-band (~ 9 GHz) were obtained in a JEOL (JES-PE-3X) spectrometer at room temperature, and the microwave power (1 mW), modulation amplitude (0.40 mT) and modulation frequency (100 kHz) were set to avoid signal
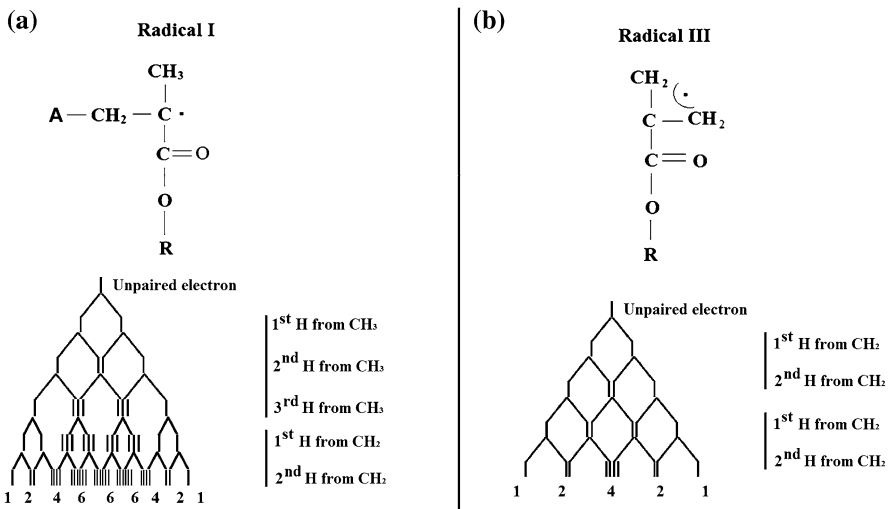
Fig. 3 a Radical I structure and the nine lines hyperfine splitting. b Radical III structure and the five lines hyperfine splitting
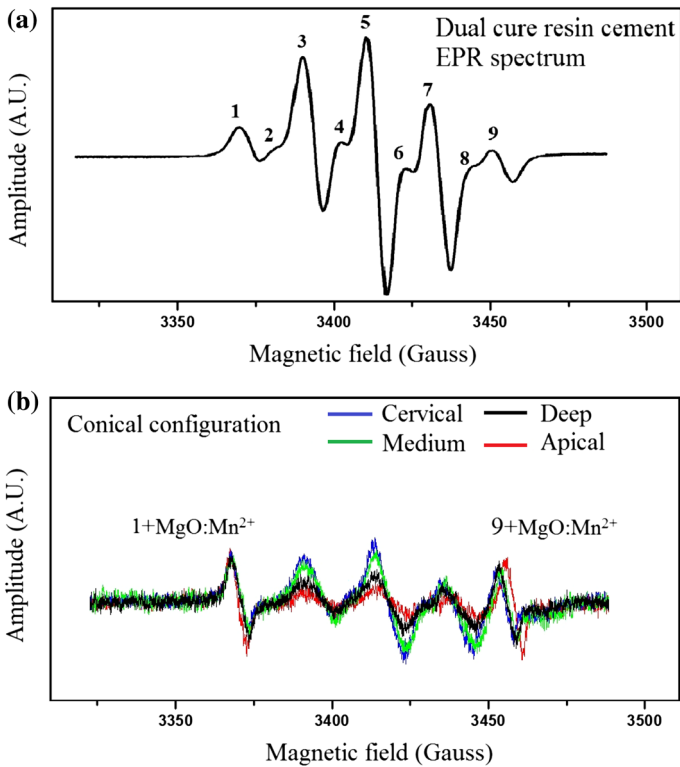
Fig. 4 a Nine line EPR spectrum of the dual-cured resin cement, characteristic of methacrylate radicals. **b** Superposition of EPR spectra obtained from the CQ, MQ, PQ and AQ of conical configuration at T_{10min}

saturation and were maintained constant. A JEOL standard sample MgO:Mn^{2+} was used as an intensity standard and *g* marker. The 2 mm samples were inserted into the EPR tube (3 mm inner diameter) and investigated immediately after 40 s of irradiation. As the EPR signal intensity is proportional to the amount of paramagnetic species in the sample and this quantity is directly related to the light incidence in the sample, it is possible to use the MgO:Mn^{2+} as the intensity standard and evaluate differences in the FR concentration for different sections of the post. Each sample was analyzed 10 min (T_{10min}) and 24 h (T_{24h}) after mixing the cement. The samples were always carefully handled with tweezers stored in aluminum packets to ensure no influence could be attributed to external light and prevent external contamination.

3 Results and Discussion

The best signal to noise ratio among the three replicate EPR spectra obtained for each sample in each experimental group was used for data treatment due to accordance between replicates (Fig. 4).

In Fig. 4, the first line is the third line of the MgO:Mn^{2+} standard superimposed on the first FR line, and the last line is the fourth resonance line of the standard superimposed on the ninth FR line. The nine lines in the EPR spectrum are typical of methacrylate radicals [17]. The EPR signal intensity for all groups was normalized with the MgO:Mn^{2+} third line intensity. In addition, the EPR signal intensity of the samples in G2 was normalized with respect to the amount of the cement mass, since the resin cement volume is not the same for all samples in this group; because the fiberglass post is conical, a reduction in diameter occurs in the cervical to apical direction. This type of normalization is not required in G1.

For data treatment, it was assumed that the relative FR concentration of the cervical sample (CQ) for G1 and G2 was 100 %, because these samples are the first surface and showed the most intense EPR signal and thus the greatest relative FR concentration. The FR concentration for all the other samples in the group was obtained relative to the CQ (Tables 2, 3).

Table 3 presents the relative FR concentrations of the samples analyzed 24 h (T_{24h}) after mixing the base paste and catalyst.

Different decay rates were observed in the relative concentrations of FR when comparing the two geometrical configurations (Table 2). The G1 MQ showed no variation in the relative concentration of FR with respect to the CQ at T_{10min}. This indicates that no significant decrease in the light transmission through the cylindrical post occurred that affected the FR concentration at depths up to 5.5 mm. In the DQ, the FR concentration was 84 % and in the AQ 70 %, clearly indicating that the effectiveness of the light transmission through the post decayed, such that the FR concentration decreased 16 % at 6–8 mm in depth and 30 % at 8–10 mm. This difference can be explained by the increase in the distance of the DQ and AQ in relation to the radiation source, even when using 1500 mW/cm^2 of power. In G2, a decrease in the FR concentration was verified for all samples compared with the CQ; the MQ, DQ and AQ decreased 11, 41 and 72 % in relative FR concentration, respectively. The distance between the LED device and the samples analyzed was a significant factor influencing the decay in FR concentration in both G1 and G2. However, for G2, the geometrical configuration also influenced light transmission through the post and thus the relative amount of FR observed in the samples tested was lower (Fig. 5).
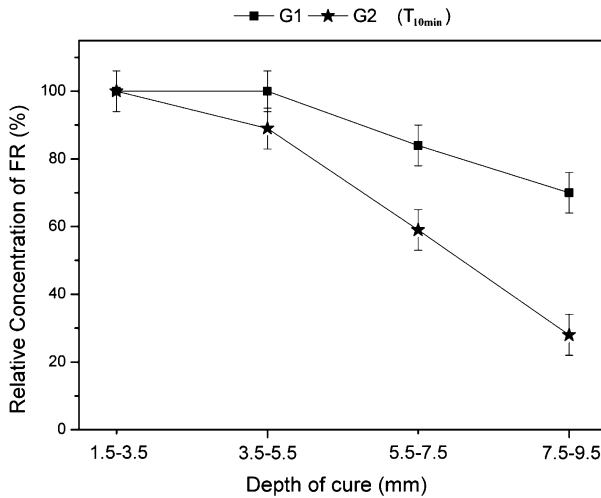
Table 2 Relative FR concentration at T_{10min}

Group	CQ (1.5–3.5 mm)	MQ (3.5–5.5 mm)	DQ (5.5–7.5 mm)	AQ (7.5–9.5 mm)
G1	100 ± 6 %	100 ± 6 %	84 ± 6 %	70 ± 6 %
G2	100 ± 6 %	89 ± 6 %	59 ± 6 %	28 ± 6 %

Table 3 Relative FR concentration at T_{24h}

Group	CQ (1.5–3.5 mm)	MQ (3.5–5.5 mm)	DQ (5.5–7.5 mm)	AQ (7.5–9.5 mm)
G1	100 ± 6 %	94 ± 6 %	98 ± 6 %	91 ± 6 %
G2	100 ± 6 %	83 ± 6 %	40 ± 6 %	14 ± 6 %

Fig. 5 Comparison of the decrease in the relative concentration of free radicals for G1 and G2 in T_{10min}

In our research, it is evident that the shape of the translucent fiberglass post influenced the transmission capacity of the light emitted from the LED device and thus the FR concentration in the dual-cured resin cement, both at T_{10min} and T_{24h}.

The diameter of ClP-1 was constant throughout the post length, as well as the amount of epoxy resin and fiberglass. However, in CnP-1, the diameter ranges from 1.6 to 1.25 mm from the cervical to the apical extremities. Considering the variation in FR concentration between G1 and G2 samples, the importance of the diameter of the post in light transmission was confirmed. This fact is consistent with the results obtained by Lui [11], who investigated the influence of post diameter relative to the depth of cure of a hybrid composite resin, inserting the post into a simulated root canal. In his research, the results showed that the larger the post diameter the better the results of polymerization of the composite resin at greater canal depth. Regarding the actual effectiveness of transmission of the light emitted by the LED device and its influence on the degree of conversion of FR in resin cement throughout the length of the cemented post, Shadman et al. observed that a translucent quartz fiber post permitted a greater degree of conversion in dual-cured cement compared with an opaque post [3]. The authors suggested that this result could be related to the difference in refractive index between glass fiber and epoxy resin in the post. When the light passes through the fiber, it crosses the resin-fiber interface at a higher angle of incidence, which allows reflection to other fibers, resulting in an increase in total light transmittance.

The behavior of light rays emitted by the LED device through interfaces with different refractive indexes could explain the results observed in G1 (Table 3), where the DQ showed a higher relative FR concentration compared with the MQ. A portion of the radiation may have been transmitted through the fiberglass and epoxy resin, while another part may have been absorbed by the mass of the resin cement. The light may also have been directly transmitted by cement located at the post-

matrix interface. However, this occurs at low intensity, since the greater part of the light undergoes scattering and absorption when passing from the external environment to the cement mass [20]. Due to changes in the geometrical configuration of CnP-1, the effectiveness of light transmission from the post to the cement is reduced because of the difference in refractive indices.

In relation to the post configuration for ClP-1, at T_{10min}, no difference was observed between the CQ and MQ. When analyzed at T_{24h}, the relative FR concentration in the MQ decreased 11 % compared with the CQ. Using an indirect method for evaluating the degree of conversion on a composite, Yoldas and Alaçam [21] observed that its polymerization could be achieved within the simulated root canal up to 8 mm deep when a fiberglass post with double geometrical configuration was used. This was also evidenced by Mallman et al. [13] and Silva et al. [6], who observed the dependence of degree of conversion on the depth of evaluation for adhesive systems and resin cements, when comparing the translucency of different posts.

Table 3 presents the relative FR concentrations for samples analyzed 24 h (T_{24h}) after mixing the base paste and catalyst. Compared with the CQ, G1 showed conformity between the relative FR concentrations, such that in the MQ, DQ and AQ showed 94, 98 and 91 %, respectively. A larger decrease in the relative FR concentrations was observed for G2 as the depth increased. In this group, the relative FR concentrations were 83, 40 and 14 % for the MQ, PQ, and AQ, respectively. This can be explained by the model represented in Fig. 6. During irradiation, the concentration of FR rapidly increases up to a maximum value [19, 22], depending on the concentration of initiators, depth of cure and other factors. When irradiation is terminated, the concentration of FR decreases exponentially to zero due to the consumption of FRs when converting monomers to polymers. At depths where the maximum amount of generated FRs is considerable smaller, the EPR spectra obtained 24 h after irradiation shows a relative concentration of FR that is lower than in those samples with a significantly greater concentration of FR.

The photopolymerization reaction takes place in three stages. Initiation occurs when the light is absorbed by the photoinitiator (camphorquinone), with a light
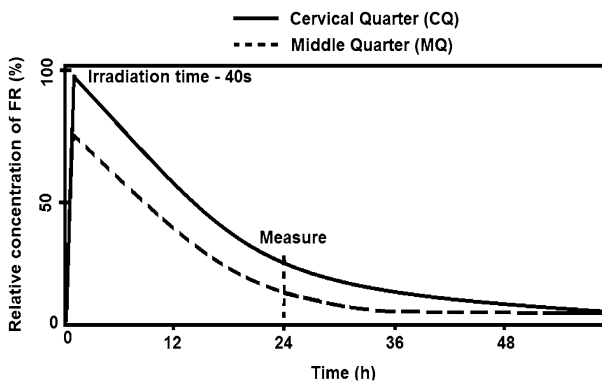
Fig. 6 Model for the behavior of the concentration of FR over time for two different depths

absorption spectrum from 400 to 500 nm. Camphorquinone reacts with active amine resulting in the formation of FRs. Next, in the propagation stage, the FRs generated bind to monomers, initiating the chain reaction. Termination occurs when the monomers with FRs bind to another active monomer, completing the polymerization reaction. However, due to vitrification of the matrix, this step may not occur, leaving a free electron in the monomer, capable of binding to other radicals [23]. Fontes et al. observed the presence of FRs in samples of composite resins polymerized for more than 70 days [22]. In the first 24 h, the process is very fast, and decelerates thereafter due to vitrification of the matrix, which restrains the termination of the polymerization reaction [22, 23]. Thus, it hardly seems unreasonable to argue that the highest concentrations of FR in all G1 samples and the upper samples of G2, at T_{24h}, occurred due to this vitrification phenomenon. However, Fontes et al. reported that the higher the concentration of FRs the better the mechanical performance, the greater the degree of conversion and depth of polymerization. Proportionality was observed between the FR concentration and quality of the resinous material, indicating that EPR spectroscopy is an important tool for understanding these dental restorative materials [22]. These data are in accordance with Salomão et al. [24]. In that case, authors studied the influence of the irradiation protocol in the depth of cure and observed that the irradiation protocol influences only in the first 8 mm of the 20-mm long double-shaped translucent fiberglass post.

4 Conclusions

Electron paramagnetic resonance spectroscopy showed that the concentration of FRs generated during polymerization is influenced by the geometrical configuration of translucent fiberglass posts. No decay was observed in the relative FR concentration up to 5.5 mm using ClP-1, which means that up to this depth of restoration, the property of light conduction in the translucent fiberglass post is effective. The diameter and anatomy of CnP-1 influenced FR formation in the dual-cured resin cement compared with the same depths using ClP-1. The cylindrical configuration is more efficient at conducting light to the deepest points of the restoration, promoting better results for post fixation.

References

1. G.M. Gomes, O.M.M. Gomes, A. Reis, J.C. Gomes, A.D. Loguercio, A.L. Calixto, Braz. Dent. J. **22**, 460–467 (2011)
2. L.F.S.A. Morgan, R.T.R.C. Peixoto, R.C. Albuquerque, M.F.S. Corrêa, L.T.A. Poletto, M.B. Pinotti, J. Endod. **34**, 299–302 (2008)
3. N. Shadman, M. Atai, M. Ghavam, H. Kermanshah, F. Ebrahimi, J. Can. Dent. Assoc. **78**, c53 (2012)
4. D.N.J. Ricketts, C.M.E. Tait, A.J. Higgins, Br. Dent. J. **198**, 533–541 (2005)

5. A.S. Fernandes, S. Sharat, I. Coutinho, J. Prosthet. Dent. **90**, 556–662 (2003)
6. A.L.F. Silva, V.G. Arias, L.E.S. Soares, A.M. Martin, L.R.M. Martins, J. Endod. **33**, 303–305 (2007)
7. L.R. Calixto, M.C. Bandéca, V. Clavijo, M.F. Andrade, L.G. Vaz, E.A. Campos, Oper. Dent. **37**, 80–86 (2012)
8. T.A. Pegoraro, N.R.F.A. Da Silva, R.M. Carvalho, Dent. Clin. N. Am. **51**, 453–471 (2007)
9. R.R. Braga, P.F. Cesar, C.C. Gonzaga, Oral Rehabil. **29**, 257–262 (2002)
10. C. Goracci, G. Corciolani, A. Vich, M. Ferrari, J. Dent. Res. **87**, 1122–1126 (2008)
11. J.L. Lui, Quintessence Int. **25**, 313–319 (1994)
12. L. Ceballos, M.A. Garrido, V. Fuentes, J. Rodríguez, Dent. Mater. **23**, 100–105 (2007)
13. A. Mallman, L.B. Jacque, L.F. Valandro, A. Muench, J. Prosthet. Dent. **97**, 165–167 (2007)
14. A.S. Fontes, W. Sano, L.H. Dall'Antonia, E. Di Mauro, Appl. Magn. Reson. **39**(4), 381–390 (2010)
15. M.A. Menezes, A. Muench, Rev. Odontol. Univ. São Paulo **12**, 281–285 (1998)
16. L.G. Lovell, K.A. Berchtold, J.E. Elliott, H. Lu, C.N. Bowman, Polym. Adv. Technol. **12**, 335–345 (2001)
17. L. Lapcik Jr, J. Jancar, A. Stasko, P. Saha, J. Mater. Sci. Mater. Med. **9**, 257–262 (1998)
18. W. Teshima, Y. Nomura, N. Tanaka, H. Urabe, M. Okazaki, Y. Nahara, Biomaterials **24**, 2097–2103 (2003)
19. A.S. Fontes, B.L.S. Vicentin, D.F. Valezi, M.F. da Costa, W. Sano, E. Di Mauro, Appl. Magn. Reson. **45**(7), 681–692 (2014)
20. F. Rueggeberg, D.M. Jordan, Int. J. Prosthodont. **6**, 364–370 (1993)
21. O. Yoldas, T. Alaçam, J. Endod. **31**, 104–106 (2005)
22. A.S. Fontes, E. Di Mauro, W. Sano, N.C.S. de Lima, L.H. Dall'Antonia, Polímeros: Ciência e Tecnologia **19**, 285–291 (2009)
23. J.G. Leprince, G. Lamblin, J. Devaux, M. Dewaele, M. Mestdagh, W.M. Palin, B. Gallez, G. Leloup, J. Dent. Res. **89**, 1494–1498 (2010)
24. F.M. Salomão, B.L.S. Vicentin, E.F.R. Contreras, M.G. Hoeppner, E. Di Mauro, Mater. Res. **18**(5), 1023–1028 (2015)